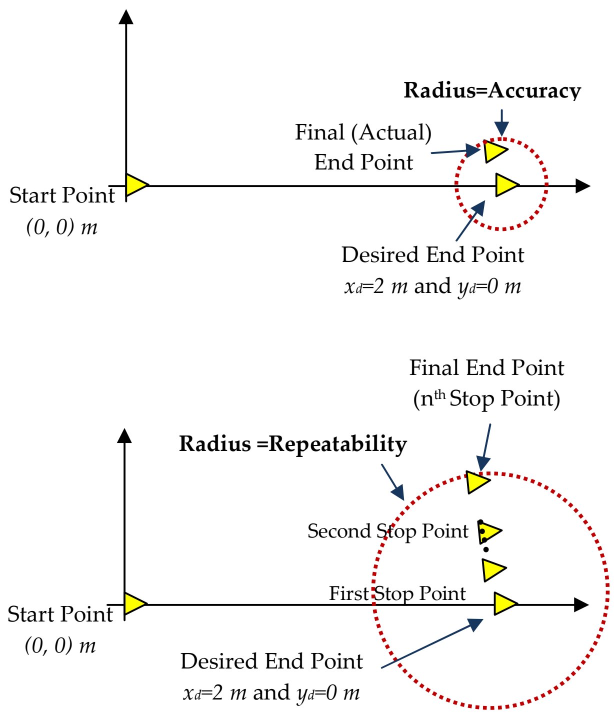

Fig.4. Defined path and related variables for accuracy and repeatability tests.

3.3. Load Capacity

Determination of load capacity of robot leads to select and attach the proper tool in end-effector. In order to determine load capacity of the robot, proper modeling of robot is a pre-requisite. Here, the computational procedure to determine the maximum allowable load capacity is outlined. To calculate the dynamic load carrying capacity of robot, after discretizing the given trajectory into *m* points, joint motion constraints, Jacobian singularity conditions and joint velocity constraints are checked [11]. In cases in which each of the constraints is violated, the given trajectory is unrealizable and a new trajectory should be selected. At next step, acceleration of each joint is found and then the dynamic equations are employed to compute the load and end-effector dynamic effects. Once the below conditions are satisfied, the value of mass carried by end-effector and related coordinate are recorded.

- *The joint kinematics variables* including the joint orientations and velocities should be bounded by two upper and lower limits:

$$\begin{cases} d_{\min,i} \le d_i \le d_{\max,i} \\ \dot{d}_{\min,i} \le \dot{d}_i \le \dot{d}_{\max,i} \end{cases} \quad (1)$$

Note that *i=1,2,3* is the joint number of Cartesian robot.

- *Non-singularity condition of robot*: Non-zero condition of Jacobian matrix for given trajectory:

$$J(d_i, \dot{d}_i, x_e, y_e, z_e) \neq 0 \quad (2)$$

where (x_e, y_e, z_e) is the coordinate of end-effector along the specific trajectory which can be a function of time.

- *Calculated torques* should be bounded too using the following equation.

$$-T_0(1+\frac{\dot{q}_i}{\omega_i}) \le T_i \le T_0(1-\frac{\dot{q}_i}{\omega_i}) \quad (3)$$

In (3), T_0 is the stall torque of each motor and depends on the characteristic of actuator, $\dot{q}_i$ denotes the full-loaded angular velocity of i^{th} motor for given path and ω_i represents the angular velocity of motor while carrying no load. Also, T_i is the torque of the i^{th} actuator.

4 Prototype Robot

Based on the process described before, a prototype model of the Cartesian robot is fabricated as shown in Fig. 5. This model is finalized after applying the changes concluded from design improvement. Also, this robot is designed on basis of the assumption in which each joint has an independent actuator with gear reduction and measuring angular joint position sensor. Mechanical elements of the robot are modelled using Solid Works software. In addition, the design of 3P robot is carried out using the design preliminary conditions (*i.e.* agreed values) and the proposed improvement algorithm to recognize and reduce the existing errors during the design and manufacturing stages [12].

4.1. Control Unit

The controller includes three drivers for three servo motors and used to drive the motors. Each motor has its own built-in reduction gears and incremental encoder. As compared to robot described in [12], the resolution of the encoders is increased from 270 p/rev to 900 p/rev. The commands are sent to the robot via the designed simulation software. This software is implemented because the manufactured robot should accomplish the given commands accurately and smoothly. This is possible in the case that the motion of the robot end-effector is accurate enough relative to the target-object that is the point that the end-effector of the manipulator has reached to. The robot works with a Pentium IV, 1600 MHz which is used for path detection algorithm processing.

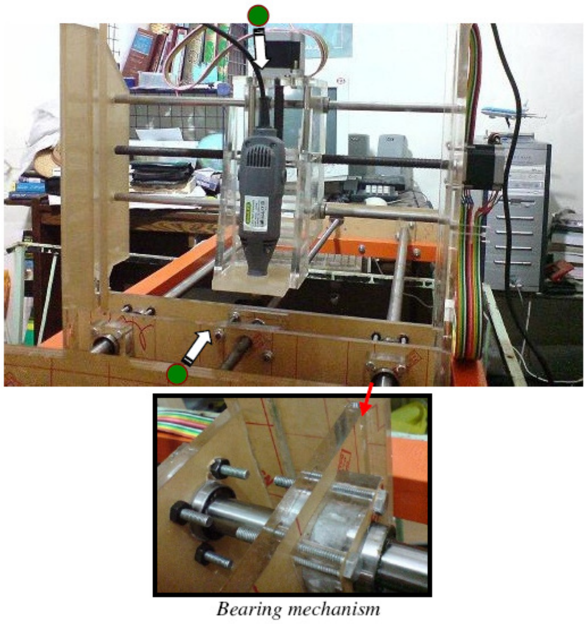

Fig.5. Manufactured 3P robot.

4.2. Interfacing Program

To transform the robot coordinates to global reference coordinate (Fig. 1), the scale section of written program is implemented. With images from these two fixed cameras, the positions of objects are shown in image plane coordinate. As shown in Figs. 5 and 6, two cameras with a certain distance from each other are looking at the end-effector. One of these two stationary cameras is fixed and zooms along Z axis (camera 1) and second one is located in Y axis direction (camera 2). Position of end-effector is determined in image plane and then is transferred to global coordinate using derived transformation matrices. Evaluation of the mentioned procedure is one of the most convenient approaches to assess the entire activity of industrial robots. Also, the measurement of described performance indices brings the opportunity of comparison the available robot with other existing robots. To make tests more applicable, the statistic analyzes are performed based on the definitions described before. As shown in Fig. 6, the cameras take the sequences of photo from object located at end-effector and the encoders read the amount of pulses of motors and the program scales the pictures and recognizes the end-effector and target situations among other objects. Then, based on the input desired path, the amount of error in X, Y and Z directions is calculated and the controller sends the compensated pulse to the motors in order to modify the motion of robot.

4.3. Mechanical Elements

The mechanical mechanism in manufactured base consists of three gearboxes and their own shafts to transmit the angular velocities of gearboxes to the axis shafts. On the bottom of the robot, covering platform is a wood plate that the work pieces are mounted on.

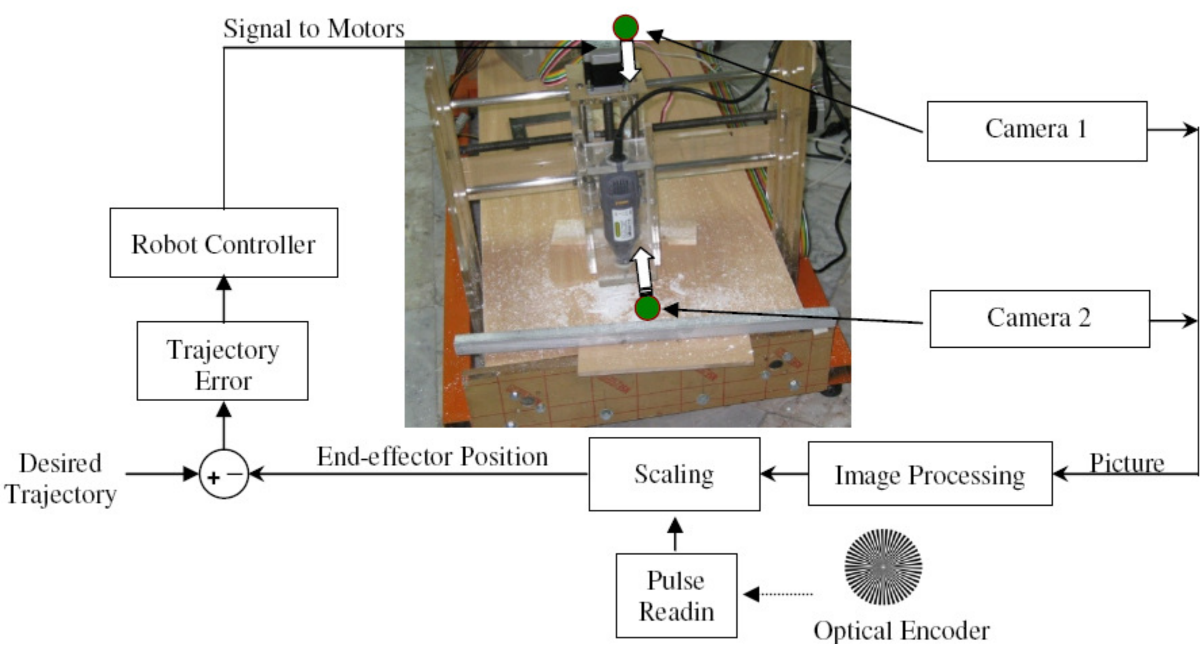

Fig.6. Position-based control structure of robot and stationary cameras (Modified from [12]).

5 Test Results

In experimental tests, first the prototype robot is tested and the performance indices are measured and compared with the agreed values. As the calculated indices in preliminary model cannot satisfy the design criteria firstly, thus, the improvement algorithm results (the required changes) are applied on robot in order to improve the design of the preliminary model. Also, the tests are repeated while some corrective actions are considered during the design and manufacturing process and the performance indices are calculated. Finally, the improvement factors are obtained and compared to the initial data. The performance tests are done using the two-camera measurement technique. As mentioned, the test parameters include accuracy, repeatability of end-effector position and load capacity of robot.

5.1. Accuracy and Repeatability: Results

Based on the described technique to posture measurement, the amount of accuracy and repeatability of robot are obtained in before and after design changes. In all experiments which are described in this section, the robot is programmed to move in a typical trajectory with *l=250 mm* in diagonal direction of *XYZ* cube which is shown in Fig. 1. In this experiment, the end-effector linear velocity is 0.12 m/s.

Figure 7 shows the mean values of experimental results obtained for accuracy and repeatability tests for given trajectory. The repeatability test is done when n=5 and n=10. The bars show the end-effector errors after and before applying the corrective actions. For each trial, this test is performed for 10 times and the end-effector error is defined as the mean value of the difference between the desired and actual positions by following equation:

$$RE = \frac{1}{10}\sum_{i=1}^{10}\sqrt{(\bar{X}_{a,i} - X_d)^2 + (\bar{Y}_{a,i} - Y_d)^2 + (\bar{Z}_{a,i} - Z_d)^2} \qquad (5)$$

where ($\bar{X}_{a,i}, \bar{Y}_{a,i}, \bar{Z}_{a,i}$) and (X_d, Y_d, Z_d) are the actual and desired coordinates, respectively. The actual coordinates are calculated using the mentioned mapping algorithm.

As illustrated in Fig. 7, the accuracy 5 time and 10 time repeatability error were reduced by 63.5%, 29.3% and 29.8%, respectively.

5.2. Trajectory Test

In next experiment, desired position of end-effector is given to robot to reach. By computing

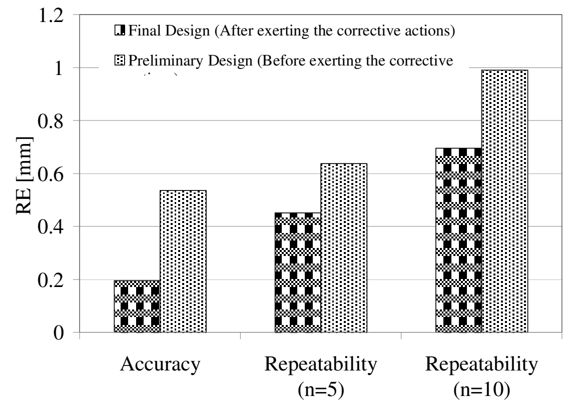

Fig.7. Error mean values of tool movement in accuracy and repeatability tests.

joint angles from inverse kinematics equations and rotation of joints, the end-effector will reach to the desired position. By taking photos with two fixed cameras, the robot equations and the counted pulses concludes the coordination of end-effector in global reference frame are determined. Also, by comparing the desired and actual amounts of end=effector position, the positioning errors are determined.

5.2.1. Quarter Circular Path

In this test, the accuracy of robot on the quarter circular continuous path is determined and the amount of error during the robot motion is calculated. The circle is in horizontal plane *i.e.* the height of robot end-effector is constant from earth level. The orientation of the end-effector doesn’t vary, thus, the end-effector is always in horizontal plane and also, normal with respect to circular path and end-effector slides along perimeter of circle. During motion of end-effector on the path, 10 images have been taken from end-effector. Using mapping system, the image coordinates of points are transformed to the reference frame. The desired and actual paths are illustrated in Fig. 8. In this experiment, the mean value of end-effector linear velocity is 0.08 m/s.

5.2.2. Straight Line

To move end-effector along a direct line, its start and end points must be determined. Approach vector direction is normal with respect to direction of line path *i.e.* end-effector is always normal to its path. With pose of end-effector and inverse kinematics equations of robot, the joint angles are computed. Joints rotate and end-effector is positioned along its path. Coordinates of end-effector in global reference frame are determined by taking pictures with two fixed cameras. The positioning error is determined by comparing the desired pose and actual one. Error of tool in traversing direct line path, when they move along *X* axis are shown in Fig. 9. The start point is coordinated by (0, 0, 0) and the final point is located on (150, 150, 150). The linear velocity of end-effector is considered to be 0.3 m/s.

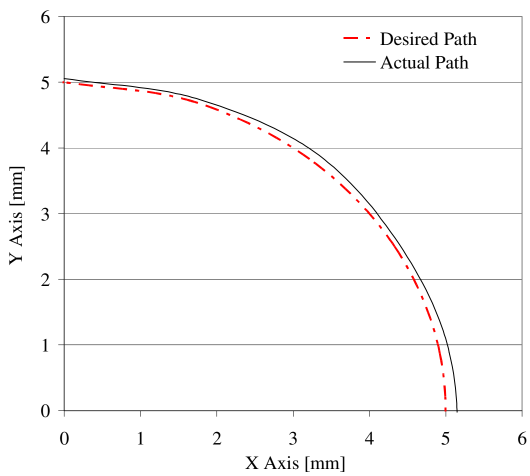

Fig.8. Desired and actual paths in quarter circular test.

5.3. Load Capacity

This section presents the calculation of the robot dynamic computations using three approaches including analytical approach, simulation study and experimental test. In all approaches, the end-effector travels from point (0,0,0) toward point (120,120,120). All experiments and simulation studies in this section are performed for final model of robot after applying the corrective actions.

5.3.1. Computational Method

In this section, the previous diagonal trajectory for the load is assumed using the algorithm presented in Section 3.3. Considering the modeling equations, the task space trajectory is descritized into equally spaced m=40 points. The allowable load carrying capacity for the mobile manipulator at every point of the trajectory is determined and maximum allowable load is found $m_{load}=8.16kg$ at point $X(t)=62.5mm$, $Y(t)=62.5mm$, $Z(t)=120mm$ as shown in Fig. 10. As shown in this section, there are some differences in the results of analytical and simulation approaches in calculation of maximum allowable load carrying capacity. The effects of friction force, load and inertia distribution types are the major reasons of this difference.

5.3.2. Simulation Approach

In this approach, the load capacity value is calculated using simulation study. Also, to determine the maximum load capacity, the model is moved in given trajectory in Working Model software and the torques of motors are derived from

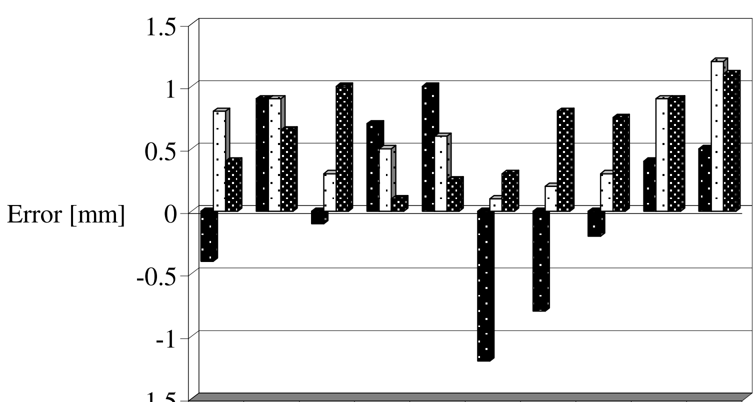

	1	2	3	4	5	6	7	8	9	10
ex	-0.4	0.9	-0.1	0.7	1	-1.2	-0.8	-0.2	0.4	0.5
ey	0.8	0.9	0.3	0.5	0.6	0.1	0.2	0.3	0.9	1.2
ez	0.4	0.65	1	0.1	0.25	0.3	0.8	0.75	0.9	1.1

Fig. 9. Error diagram in x, y, z directions in straight line trajectory applied on final design of robot which are shown by e_x, e_y, e_z, respectively.

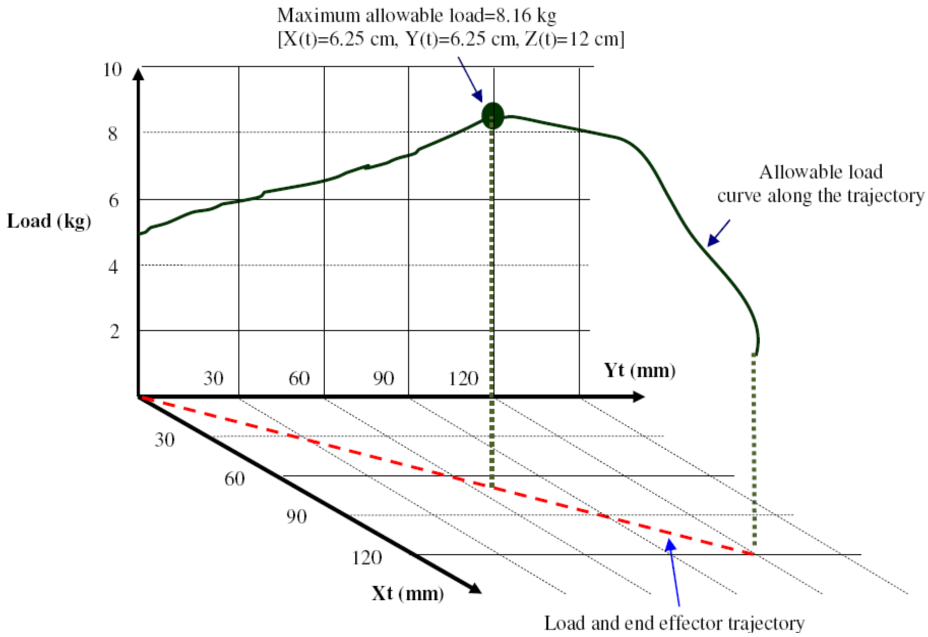

Fig. 10. Variation of allowable load along load trajectory and load capacity.

software output. In this estimation, the amount of plus load mass is increased in each trial and the torques are checked. When one of motors reaches to its critical torque, it means that robot is carrying its maximum load in given trajectory. For calculation of maximum allowable load, Cartesian robot is moved in given trajectory and the initial load is taken to zero, then the load is increased by steps of 0.1 kg. Figure 11 shows the maximum torques of motor 2 for given manipulator load in each trials.

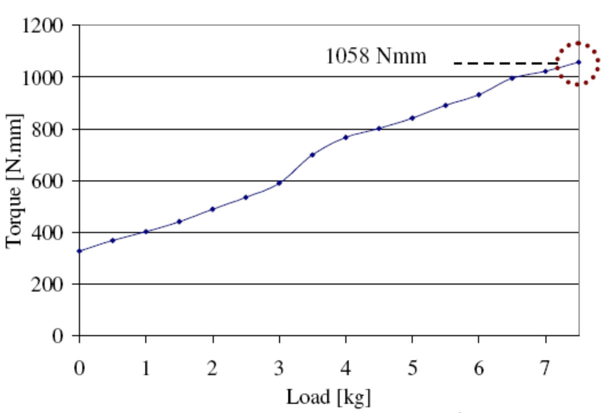

Fig.11. Torque-load variations for 2nd actuator.

As a results, according to this figure, for m_{load}=*7.5kg*, motor 2 (Y axis motor) reaches its maximum value τ=*1058 Nmm*. As shown in Fig. 11, the torque of motor 2 restricts the load capacity in end-effector and the maximum allowable load for given trajectory is determined as $m_{allowable}$=*7.5kg*. In this estimation, some disturbances neglected in theoretical modeling take into account such as the effect of friction forces, unsymmetrical distribution of robot mass and probable misalignments in joints. This consideration makes the results more accurate as opposed to analytical approach.

5.3.3. Experimental Approach

In this approach, the amount of torque for each motor is derived using laboratory tests applied on this robot. The obtained data are perfectly experimental and all existing errors sources such as friction effects have been considered. The amount of maximum load capacity for this path is obtained about *5.64kg* using three torque-meters installed on the actuators (Fig. 11). The implemented digital torque meters are made by Shenzhen Tony Electronics Company and named SHITO. They are the intellectualized instruments for measuring and setting torque which are mostly used for inspecting the torque of electric torque drivers and used to measure the torque produced during the actuators motions. These sensors are designed as easy-to-operate, accurate, functional and portable tools.

6 Statistical Analysis

In order to compare the obtained results with the agreed values in design stage, the calculated indices based on the data resulted from experiments are considered according to Table 1. As shown in this

Table 1- Experimented Indices Values.

	DLCC (kg)	Mean Accuracy (mm)	Mean Repeatability 5 times (mm)	Mean Repeatability 10 times (mm)
Agreed Values	5.00	5	10	15
Preliminary Design	3.21	10.70	12.75	19.80
Final Design	5. 64	3.91	9.01	13.90

table, all derived data are acceptable and also, confirm the final design based on the agreed values. Thus, the changes applied during the design process are reasonable in the sense of defined and agreed indices.

7 Conclusions

This paper addressed the procedure of experimental evaluation and improvement of the design and application of Cartesian robots by implementing the experimental tests. This design was completed based on some predefined indices which can be obtained using experimental tests. These indices were specified during the design process as design inputs according to the anticipated workability of Cartesian robots. These performance indices consist of the accuracy, repeatability and load carrying capacity. In addition, in order to validate the described procedure, a prototype model of Cartesian robot was manufactured and tested. Then, after exerting changes during design process (mentioned in [12]), the experiments showed great improvement over the preliminary design of robot. For example, the accuracy, 5 time and 10 time repeatability errors were reduced by 63.5%, 29.3% and 29.8%, respectively.

References

[1] S.D. Timar, R.T. Farouki, T.S. Smith, & C.L. Boyadjieff, Algorithms for time-optimal control of CNC machines along curved tool paths, *Robotics and Computer Integrated Manufacturing*, 21, 2005, 37–53.

[2] P.S. Snches, & F.R. Cortes, A New Cartesian Controller for Robot Manipulators, *IEEE/RSJ International Conference on Intelligent Robots and Systems*, 2005, 3536-3542.

[3] A. Azhdari, N. G. Chalhoub, & F. Gordaninejad, Nonlinear Dynamic Modelling of a Revolute-Prismatic Flexible Composite-Material Robot Arm, *Journal of Vibration and Acoustics*, *113* (4), 1991, 461-468.

[4] A. G. Reynoso, Structural dynamic model of a Cartesian robot, *MIT Artificial Intelligence Laboratory,* PhD Thesis, 1967.

[5] F. Heinz, B. Dennis, M. Marcus, M. Anton, N. Gregor, & M. Stefan, Optimized control methods for capturing flying objects with a Cartesian Robot, *IEEE Int. Conf. on Robotics, Automation and Mechatronics*, 2008, 160-165.

[6] H. Ghorabi, Y. Maddahi, S. M. Hosseini Monsef, & A. Maddahi, Design and Experimental Tests of a Pick and Place Robot: Theoretical and Experimental Approaches, *International Conference on Applications of Electrical Engineering*, Malaysia, 2010.

[7] Massimo Callegari, Ferdinando Cannella, Sergio Monti, Claudio Santolini, & Paolo Pagnanelli, Dynamic Model for a Re-Engineering of a High-Speed Cartesian Robot, *IEEE/ASME International Conference on Advanced Engineering Mechatronic*, Italy, 2001, 560-565.

[8] Cheng, H.H., Lee, J.J., & Penkar, R., Kinematic analysis of a hybrid serial-and-parallel-driven redundant industrial manipulator, *International Journal of Robotics and Automation, 10*(4), 1995, 159-166

[9] L. T. Wang, & B. Ravani, Dynamic load carrying capacity of mechanical manipulators-Part 1: Problem formulation, *Journal of Dyn. Sys. Meas. and Control, 110*, 1988, 46-52.

[10] Timar, S.D., Farouki, R.T., & Boyadjieff, C.L., Time-optimal feed rates along curved paths for cartesian CNC machines with prescribed bounds on axis velocities and accelerations, *International Journal of Robotics and Automation, 22*(2), 2007, 112-125.

[11] Y. Maddahi, Calculation of Load Carrying Capacity on a Redundant Manipulator, *International Conference on* Circuits, Systems, Signal and Telecommunications, Mexico, 2008.

[12] Y. Maddahi, N. Sepehri, H. Ghorabi and A. Maddahi, "Testing Robotic Manipulator: Improvement and Experience", *International Journal of Systems Applications, Engineering and Development*, pp. 35-45, 2010.

[13] R. Qiang, Research on Sales Quality System Improvement Based on FMEA. *International Conference on Service Systems and Service Management*, China, pp. 905 – 909, 2009.